IEEE Access
Multidisciplinary | Rapid Review | Open Access Journal

Received June 22, 2020, accepted July 2, 2020, date of publication July 13, 2020, date of current version July 24, 2020.

Digital Object Identifier 10.1109/ACCESS.2020.3008966

A Compact and Straightforward Self-Decoupled MIMO Antenna System for 5G Applications

HAIYAN PIAO[1], YUNNAN JIN[1], (Member, IEEE), AND LONGYUE QU[1,2], (Member, IEEE)
[1]Department of Electronics and Computer Engineering, Hanyang University, Seoul 04763, South Korea
[2]School of Electronics & Information Engineering, Nanjing University of Information Science & Technology (NUIST), Nanjing 210000, China

Corresponding author: Longyue Qu (rioinkorea@gmail.com)

This work was supported in part by the China Scholarship Council (CSC), and in part by Hanyang Antenna Company Ltd., Shenzhen, China.

ABSTRACT This study investigates a compact and straightforward self-decoupled 2 × 2 multiple-input multiple-output (MIMO) antenna set and its applications for current and future 5G terminal devices. The proposed self-decoupled MIMO antennas include a popularly used loop antenna and a compact loop-type ground-radiation antenna without utilizing any supplementary decoupling structures or undergoing complex tuning process. It is revealed that the loop antenna and the ground-radiation antenna can be modeled as an electric-current element and a magnetic-current element, respectively. This orthogonality allows the self-decoupled characteristic of the proposed MIMO antennas even though the antenna elements are tightly arranged and collocated together. An 8 × 8 MIMO antenna system is further demonstrated for 5G MIMO applications, where both simulation and measurement are conducted to validate the feasibility of the proposed technique. It is concluded that the proposed MIMO antenna system is a smart way to generate high isolation and low correlation characteristics while having advantages of low profile and easy fabrication so that it can be recognized as a promising candidate for 5G applications.

INDEX TERMS Multiple-input multiple-output (MIMO), 5G, terminal devices, loop antenna, ground-radiation antenna, orthogonality.

I. INTRODUCTION

Multiple-input multiple-output (MIMO), utilizing multiple antenna elements for simultaneous transmission and reception at the same radio channel without increasing the input power or frequency spectrum, is a critical technology to increase the channel capacity and provide high data rate for 4G Long-Term Evolution (LTE) applications and the next generation wireless communication (5G) [1], [2]. With the popularization of the 4G communication system, LTE and LTE-Advanced systems have been deployed so fast with the ability to support data rates of 100 Mb/s to 1 Gb/s. However, the proliferation of user numbers and an explosion of more powerful cellular devices, demanding high-quality video and multimedia applications, lead to an avalanche of wireless traffic. Therefore, 5G is proposed to support ultra-fast speeds (up to multiple gigabits per second with a minimum user experienced data rate of one gigabit per second), low latency, and excellent reliability while supporting massive machine-type communications [3], [4]. As one of the most innovative and practical solutions to realize the aforementioned 5G vision, the use of a vast amount of underutilized spectrum in the 3–300 GHz has gained significant interest. Of the 5G new radio spectrum, the sub-6 GHz bands can achieve the best compromise between capacity and coverage, not easily being interfered by walls, trees, and other obstacles.

With the allocation of the 3.5 GHz (3.4–3.6 GHz) band for 5G wireless communication [5], the sub-6 GHz MIMO antenna systems have been popularly studied to allow more antenna elements to be integrated into space-scarce terminal devices [6]–[23]. It has been demonstrated that high isolation (i.e., low mutual coupling) and low correlation are essential figure-of-merits for MIMO antenna systems to guarantee excellent radiation performance and diversity property. Moreover, terminal antennas with compact volume, simple installation, and cost-effective fabrication, are of great interest because terminal antennas are often accompanied by the harshest requirements and the worst implementation circumstances. Therefore, integration of large-scale sub-6 GHz antenna elements into the crowd terminal devices

The associate editor coordinating the review of this manuscript and approving it for publication was Sudipta Chattopadhyay.

while maintaining high performances is the first and foremost issue because their wavelengths are still comparable to those in current 4G systems.

In the literature, the previously reported techniques for the sub-6 GHz 5G MIMO antennas can be categorized into the following two categories: decoupled MIMO antenna arrays by utilizing decoupling structures [6]–[12] and self-decoupled MIMO antenna arrays without any additional structures [13]–[23]. For the decoupled MIMO antenna arrays, the frequently adopted decoupling structures include neutralization lines or decoupling networks [6]–[9], and additional resonators [9]–[12], which require additional occupation and complicated tuning efforts. On the contrary, the self-decoupled MIMO antenna arrays can achieve adequate isolation by proper arrangement [13]–[17] and polarization or pattern control [18]–[23], circumventing the case-by-case implementation of extra decoupling structures. However, some of them require vast distances between each two antenna elements [13]–[17], which severely limit the scale of the integrated antennas; in contrast, others suffer from structural complexity, implementation difficulty, or constrained position requirements. Therefore, compact and straightforward self-decoupled MIMO antennas with simple structures and cost-effective implementation is favorable in practical applications.

Furthermore, ground-radiation antennas [24]–[30] are reported as small loop-type resonators, occupying ultra-small ground clearance, and exciting the conducting body for radiation. Although they have been widely applied in terminal devices, such as laptops, smartphones, Internet of Things (IoT) devices, their MIMO applications are not compact at all [27], [30] so that they are not suitable in 5G MIMO scenarios. This motivates this paper to investigate a simple and efficient MIMO technique for ground-radiation antennas to suit current and future terminal devices.

In this study, a self-decoupled MIMO antenna set [31] is accomplished by merely integrating a popularly used loop antenna [32]–[34] with a conventional ground-radiation antenna. It is revealed that the loop is equivalent to an array of two parallel electric-current sources, and the ground-radiation antenna is equivalent to a magnetic-current source; this orthogonality contributes to the high isolation property with no need for any additional structural support or tuning efforts. The rest of this manuscript is organized as follows. In Section II, the proposed self-decoupled 2 × 2 MIMO antenna set is described. Additionally, the operation mechanism is explained, and further study of various implementation cases is also discussed. In Section III, an 8 × 8 MIMO antenna array is evaluated in simulation and measurement to verify the proposed technique for 5G applications.

II. SELF-DECOUPLED 2 × 2 MIMO ANTENNA SET

A. ANTENNA CONFIGURATION

Figure 1 depicts the proposed self-decoupled 2 × 2 MIMO antenna set, which is accomplished by combining a typically used loop antenna with a conventional loop-type ground-radiation antenna. As shown, the proposed MIMO antennas are installed on a 140 mm × 70 mm ground plane, which is etched in a 0.8-mm-thick FR4 substrate ($\varepsilon_r = 4.4$, $\tan\delta = 0.02$).

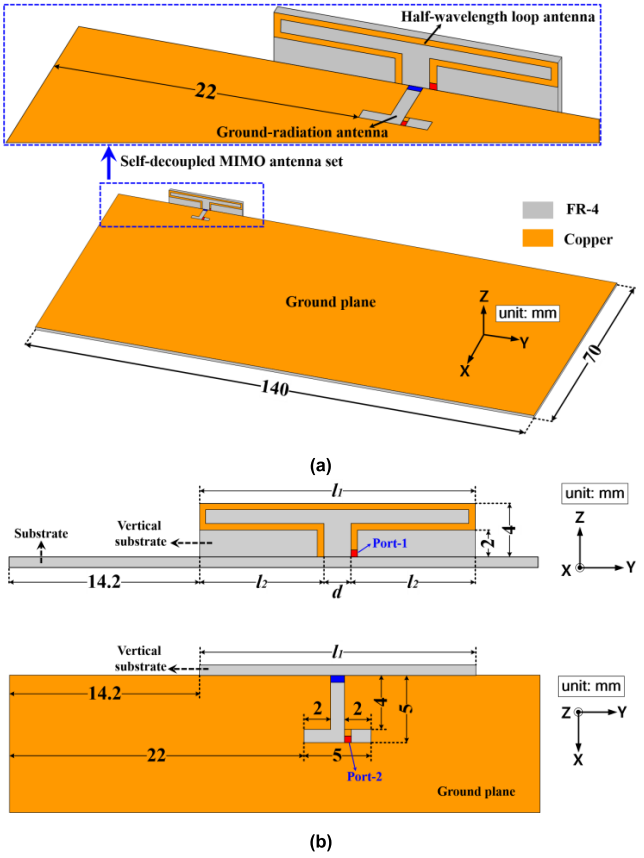

FIGURE 1. Antenna configurations of the proposed self-decoupled MIMO antenna set: (a) perspective view, and (b) side view.

The loop antenna (Antenna-1) is vertically constructed in the *yz*-plane and has a symmetrical structure etched on a 0.8-mm-thick FR4 substrate. It is directly fed by a voltage source at one end and shorted to the ground plane at the other end, thus producing current maximums at its two end portions and current nulls at its center portion [32]–[34], thus the electrical length of the loop antenna is about 0.5 wavelength. The loop antenna is popularly utilized in terminal devices because its input impedance can be varied over a wide range of values to match the characteristic impedance of the transmission lines [35]. The upper horizontal strip and the lower horizontal strip have lengths of l_1 (20.6 mm) and l_2 (9.3 mm), respectively; the edge-to-edge distance between two ends of the antenna structure (d) is 2 mm. Accordingly, the overall dimension of the proposed loop antenna is 4 mm × 20.6 mm × 0.8 mm.

The ground-radiation antenna is designed within a 1 mm-wide T-shaped clearance of the ground plane. A voltage source is utilized for excitation and impedance matching of the ground-radiation antenna, and a resonance capacitor C_r (0.29 pF) is adopted at the open end of the clearance

for convenient control of the antenna's resonant frequency. The resonance capacitor C_r not only can dramatically miniaturize the antenna area but also can control the antenna's resonance without modifying the antenna's dimensions. In this way, a miniature loop-type resonator can be formed around the clearance, operating as a magnetic coupling element to the ground plane for radiation [24]–[30]. As can be observed, the two ends of the loop antenna are symmetrically installed on the two sides of the open end of the ground-radiation antenna, establishing the proposed self-decoupled 2 × 2 MIMO antenna set without any additional decoupling structures. Note that the width of all conductor lines is 0.5 mm, and more information can be referred to in Fig. 2.

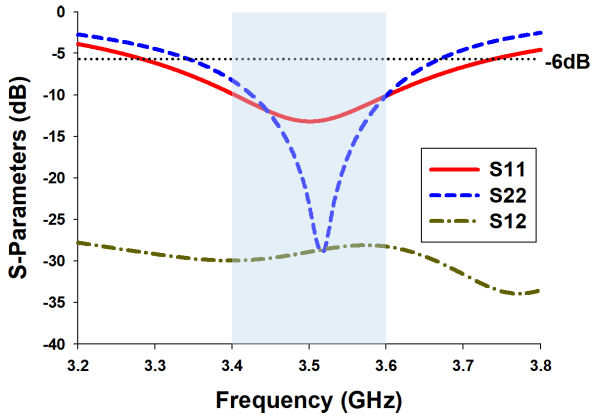

FIGURE 2. Simulated S-parameters of the proposed self-decoupled MIMO antenna set.

B. SIMULATION RESULTS AND OPERATION MECHANISM

The simulated scattering parameters (S-parameters) are presented in Fig. 2, where it can be observed that wideband characteristics and high isolation are generated. As shown in the S_{11} and S_{22} curves, the 3:1 VSWR bandwidths of the loop antenna and the ground-radiation antenna are 430 MHz (from 3.3 to 3.73 GHz) and 310 MHz (from 3.35 to 3.66 GHz), respectively, fully covering the target frequency band. As observed in the S_{12} curve, the mutual coupling over the whole frequency band is lower than −28 dB, indicating the high isolation property of the proposed self-decoupled MIMO antenna set. Therefore, the assembly of the loop antenna and the ground-radiation antenna is a smart way that can introduce the self-decoupling effect without any additional structural support and complicated tuning efforts.

Figure 3 presents the simulated S_{22} curves with the variation of the capacitor values of C_r to further clarify the operation principle of the ground-radiation antenna. As shown, the resonant frequency of the ground-radiation antenna is lowered down from 5.5 GHz to 3.5 GHz as the capacitor value of C_r is increased to 0.29 pF. This is the case because the ground-radiation antenna can exploit the inductance from the ground body around the clearance and the capacitance from the loaded capacitor to form a loop-type resonant circuit.

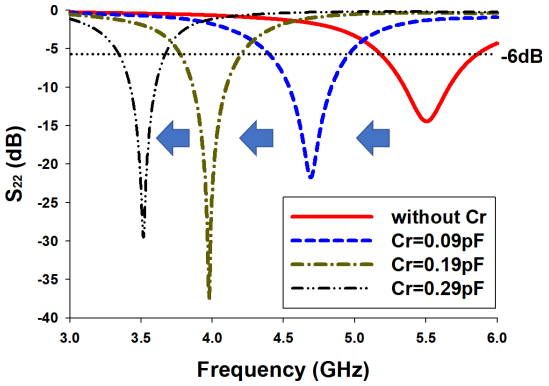

FIGURE 3. Simulated S_{22} curves with the variation of the capacitor C_r of the ground-radiation antenna.

In this way, the resonant frequency of the ground-radiation antenna can be conveniently controlled only by adjusting the capacitor value without changing the clearance area. More information on the ground-radiation antenna can be referred to [24]–[30].

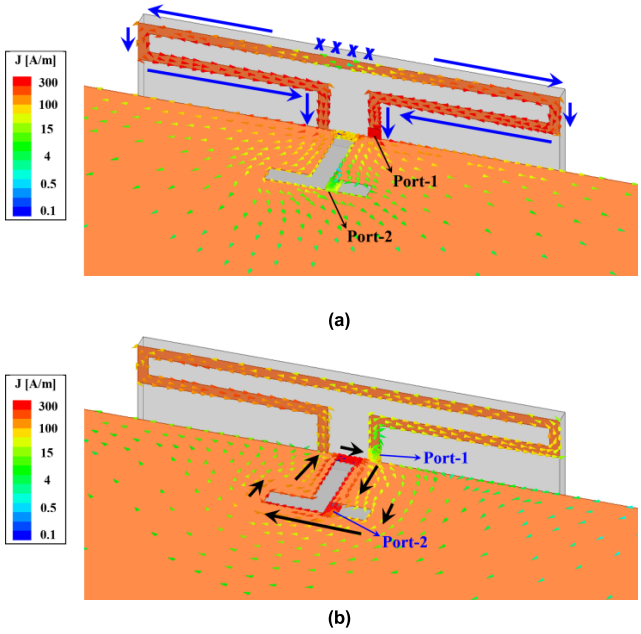

FIGURE 4. Simulated surface current distributions of the proposed MIMO antenna set at 3.5 GHz: (a) with excitation of the loop antenna, and (b) with excitation of the ground-radiation antenna.

To better understand the operation mechanism of the proposed self-decoupled MIMO antenna set, the simulated surface current distributions at 3.5 GHz are displayed in Fig. 4 for a clear observation of the operating current modes. As shown in Fig. 4(a), the loop antenna produces current maximums at the two end portions and a current minimum at its center portion (denoted by crosses in the figure), which resembles the fundamental current mode of a loop antenna. Alternatively, a small loop-type current mode, flowing around the clearance and through the

resonance capacitor C_r, is generated by the ground-radiation antenna, as can be observed in Fig. 4(b). In this way, the ground-radiation antenna is operating as a magnetic coupling element and exciting the ground plane for far-field radiation, just as the name of the ground-radiation antenna implies. Additionally, the induced currents from one port to another are extremely weak, verifying the high isolation property between the two antenna elements.

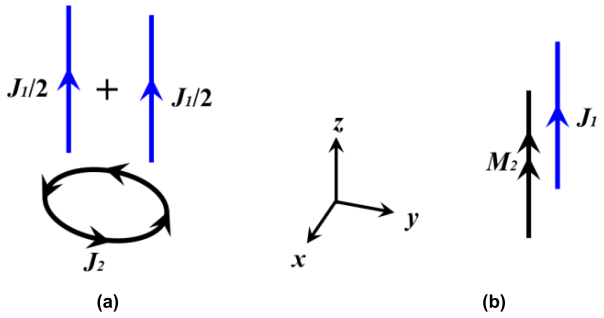

FIGURE 5. Operation mechanism of the proposed self-decoupled MIMO antenna set: (a) modeled current sources, and (b) equivalent current sources.

To further understand the operation mechanism of the proposed self-decoupled MIMO antenna set, more explanation is illustrated by the modeled current sources of the antenna elements, as shown in Fig. 5. The loop antenna can be modeled as an array of two parallel electric-current sources placed in the *yz*-plane, which is then equivalent to a dipole-type electric-current element ($\boldsymbol{J}_1$) along the *z*-axis. Whereas, the ground-radiation antenna can be modeled as a small loop-type electric-current source ($\boldsymbol{J}_2$) in the *xy*-plane, which is then equivalent to a magnetic-current element ($\boldsymbol{M}_2$) along the *z*-axis. Accordingly, the radiated electric fields from $\boldsymbol{J}_1$ are orthogonal to those from $\boldsymbol{M}_2$; this orthogonality characteristic between the two current elements ensures the high isolation characteristic between the two antennas, allowing successful implementation of the proposed self-decoupled MIMO antenna set.

C. PLANAR DESIGN

Alternatively, a planar design of the proposed self-decoupled MIMO antennas is constructed by disposing of the loop antenna in the same plane as the ground-radiation antenna (i.e., the *xy*-plane), as shown in Fig. 6(a).

The loop antenna (Antenna-1) is horizontally constructed in the *xy*-plane and has a symmetrical structure etched on a 3 mm × 21 mm × 0.8 mm FR4 substrate. The ground-radiation antenna has the same configuration as the one in Fig. 1, which is designed within a 1 mm-wide T-shaped clearance with a resonance capacitor C_r (0.31 pF). As shown, the loop antenna is symmetrically installed outside of the ground-radiation antenna, establishing a planar design of the proposed self-decoupled MIMO antenna set.

The simulated S-parameters are presented in Fig. 6(b), where it can be verified that the planar design produces

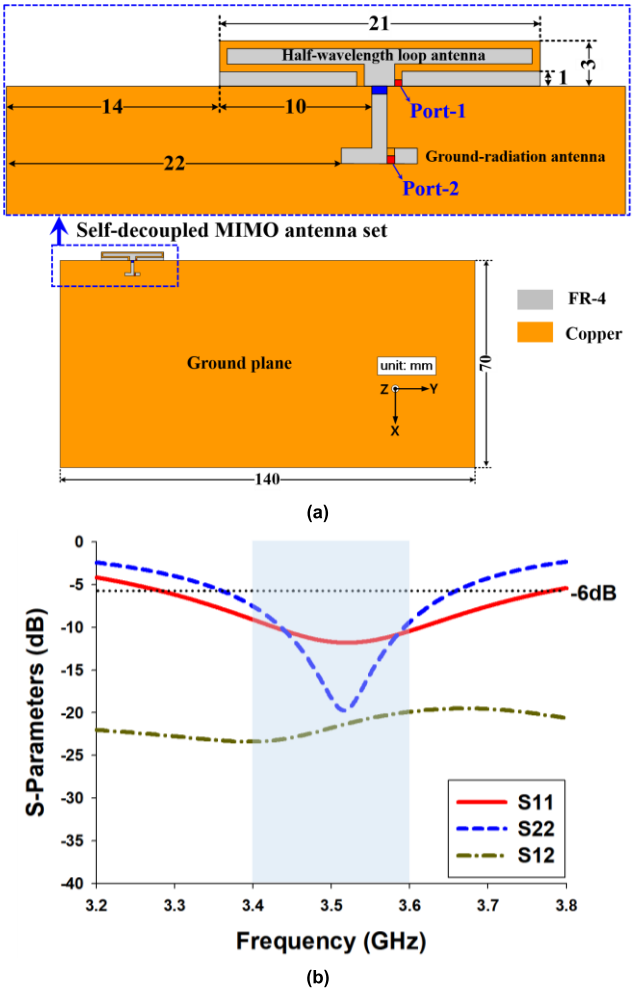

FIGURE 6. Planar design of the proposed self-decoupled MIMO antennas: (a) antenna configurations, and (b) simulated results.

broadband impedance bandwidths and high isolation property. Therefore, both the original design in Fig. 1 and the planar design in Fig. 6 are suitable for 5G applications.

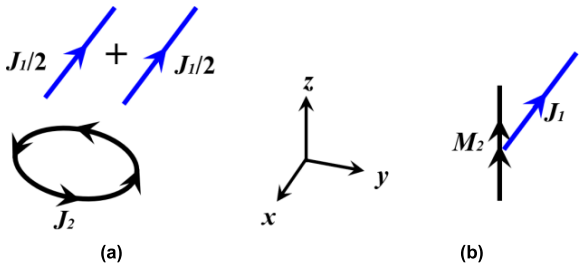

FIGURE 7. Operation mechanism of the planar design of the proposed self-decoupled MIMO antenna set: (a) modeled current sources, and (b) equivalent current sources.

The modeled current sources of the planar design of the proposed self-decoupled MIMO antennas are shown in Fig. 7. In this case, the modeled array of two parallel electric-current sources in the *xy*-plane is equivalent to an electric-current element ($\boldsymbol{J}_1$) directed to the *x*-axis.

Accordingly, the z-directed magnetic-current element $\boldsymbol{M}_2$ and the x-directed electric-current element ($\boldsymbol{J}_1$) also have orthogonality property. Accordingly, the loop antenna can be implemented at any plane to tailor various construction requirements, which can be an attractive feature in practical scenarios.

D. FURTHER STUDY AND DISCUSSION

This subsection discusses other implementation cases of the proposed self-decoupled MIMO antenna set to validate its functionality and feasibility. Here, three cases are studied by varying the structures of the loop antenna while maintaining the structural parameters of the ground-radiation antenna.

In Case 1, the edge-to-edge distance between the two ends of the loop antenna (d) is expanded to 6 mm (see Fig. 8(a)). The upper and lower horizontal strips (l_1 and l_2) are adjusted as 23.2 and 8.6 mm, respectively, to match the resonant frequency. It can be observed that the isolation between the two antenna elements is over 19 dB while the impedance characteristics are barely changed. Figure 8(b) displays the antenna configurations and simulated results of Case 2, where the edge-to-edge distance (d) is expanded to l_2 mm. In this case, the upper and lower horizontal strip (l_1 and l_2) are correspondingly adjusted as 26.6 and 7.3 mm, respectively. It can be seen that only a slight perturbation is engendered in the reflection coefficients and the transmission coefficient.

Additionally, a particular case is presented in Fig. 8(c), where a simple rectangular loop structure is used to constitutes the loop antenna with a length of 30 mm, i.e., $l_1 = 30$ mm. Accordingly, the loop antenna is transformed into a 30 mm $\times$ 4 mm rectangular loop that is directly fed by a voltage source at the right end. Still, the obtained isolation between the two antenna elements is higher than 19 dB; however, the reflection coefficient of the loop antenna deteriorates significantly due to the over-coupled impedance matching. It is noted that, in all three cases, the ground-radiation antenna is located at the center of the loop antenna, exhibiting almost unchanged impedance characteristics.

The insertion of a shorting pin is a well-known method to manipulate the input impedance characteristics of the loop antenna. Accordingly, an alternative implementation case of the proposed self-decoupled MIMO antennas, evolved from Case 3, is presented in Fig. 9(a). The loop antenna has a dimension of a 32.2 mm $\times$ 4 mm, and a shorting pin is adopted at the right side of the feed point for impedance matching. It is noted that the ground-radiation antenna is still located at the center portion of the loop antenna for consideration of an optimized self-decoupled effect. The simulated S-parameters are displayed in Fig. 9(b); as can be verified, both antennas can produce sufficient impedance bandwidths to cover the operating frequency band fully, and the mutual coupling between the two antennas is lower than -15 dB.

Therefore, the proposed self-decoupled MIMO antenna set is a simple yet efficient method to accomplish compact MIMO antennas in various forms, thereby suitable for different application scenarios. Furthermore, the unique

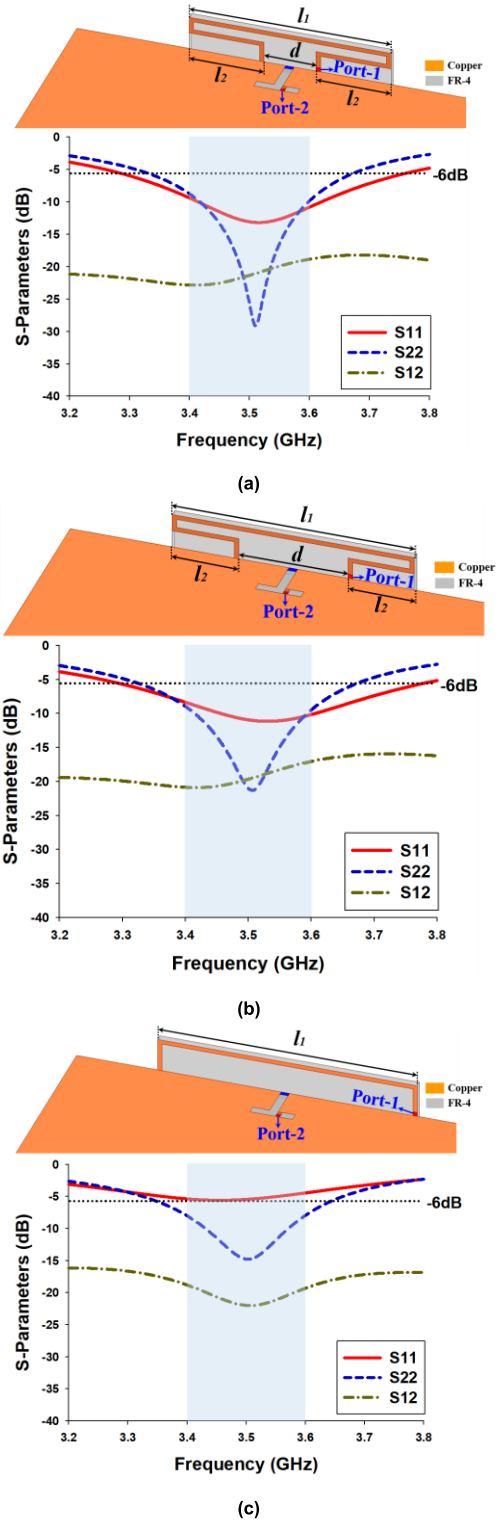

FIGURE 8. Various implementation cases of the proposed self-decoupled MIMO antenna set: (a) Case 1, (b) Case 2, and (c) Case 3.

orthogonality between the loop antenna and the ground radiation antenna also ensures their stable performance regardless of their location with respect to the ground plane, which is not discussed here. Additionally, further study is undergoing, for example, a comprehensive analysis of the interaction

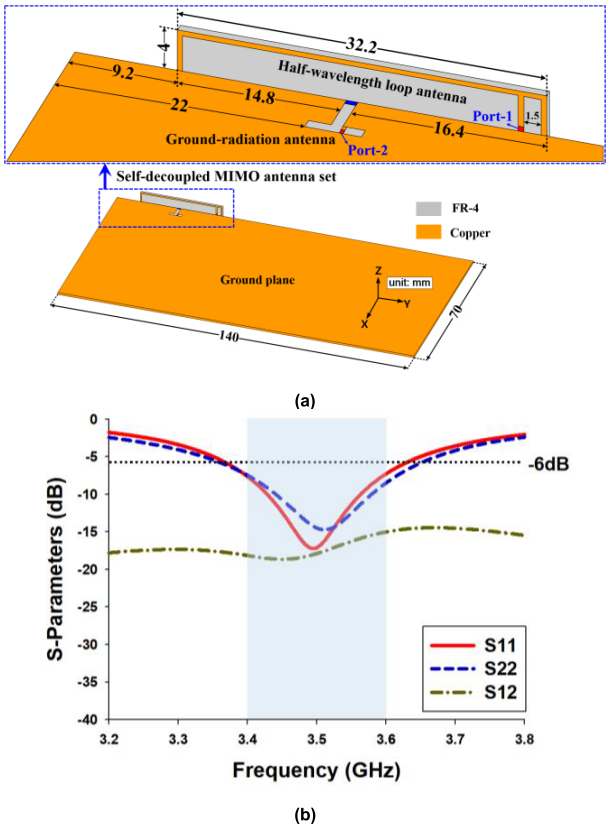

FIGURE 9. Alternative implementation case of the proposed self-decoupled MIMO antennas: (a) antenna configurations, and (b) simulated results.

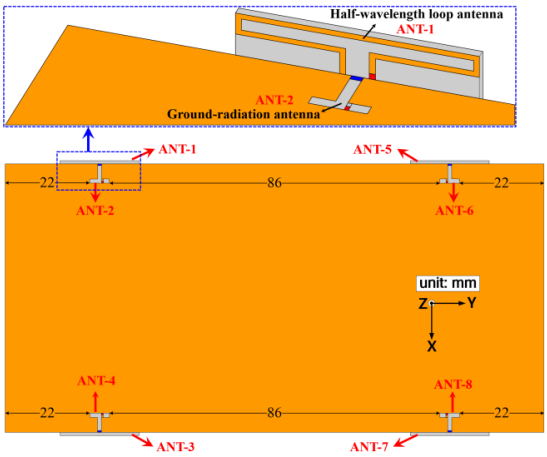

FIGURE 10. Configurations of the proposed 8 × 8 MIMO antennas for 5G applications.

between the ground-radiation antenna and the components in the terminal devices (e.g., the display and the metal frame) is under study.

III. DEMONSTRATION OF 8 × 8 MIMO ANTENNA SYSTEM

A. ANTENNA CONFIGURATION AND SIMULATION RESULTS

Generally, the 5G MIMO antennas can be arranged along the long sides of the ground plane to leave space for

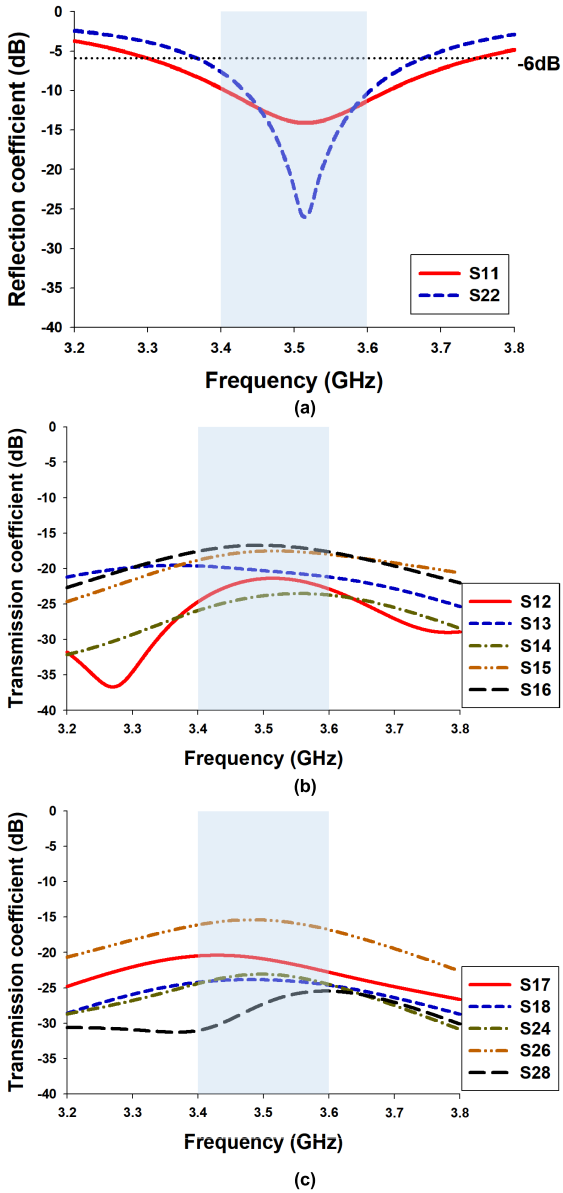

FIGURE 11. Simulated S-parameters of the proposed 8 × 8 MIMO antennas: (a) reflection coefficients, (b) and (c) transmission coefficients.

the implementation of 3G/4G antenna systems. Meanwhile, the proposed self-decoupled 2 × 2 MIMO antenna set can be duplicated into terminal devices to simply accomplish an N × N MIMO antenna system for current and future 5G MIMO applications. Accordingly, an 8 × 8 MIMO antenna system is presented in Fig. 10 as a case study to verify the feasibility of the proposed technique. The proposed 8 × 8 MIMO antenna system is comprised of four symmetrically arranged 2 × 2 MIMO antenna sets, and detailed information can be found by referring to Fig. 10. It is important to note that the edge-to-edge distance between two ground-radiation antenna elements at the same side of the ground plane is larger than one wavelength (86 mm), so self-decoupling effects between each two 2 × 2 MIMO antenna sets are also guaranteed due to spatial separation.

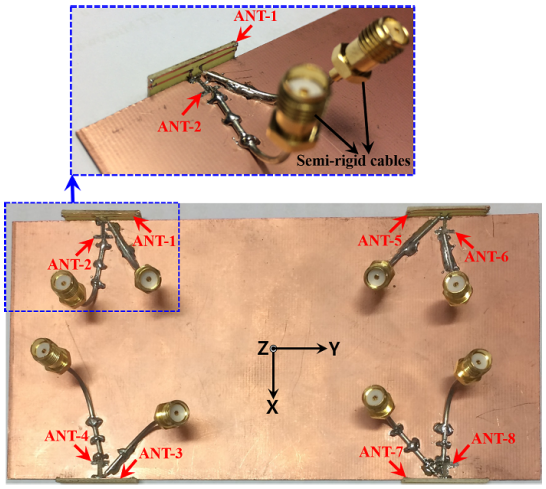

FIGURE 12. The prototype of the fabricated 8 × 8 MIMO antennas.

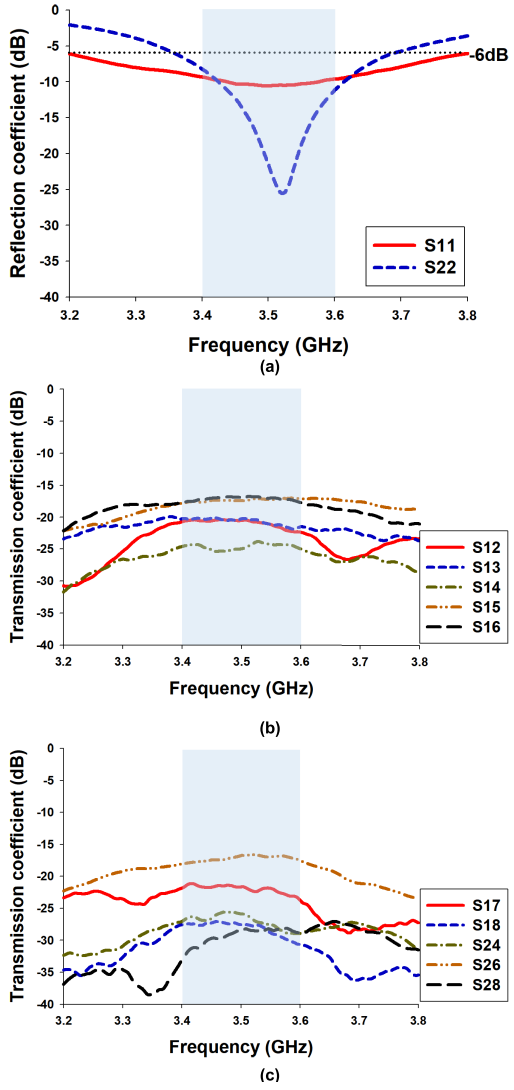

FIGURE 13. Measured S-parameters of the fabricated 8 × 8 MIMO antennas: (a) reflection coefficients, (b) and (c) transmission coefficients.

The simulated S-parameters of the proposed 8 × 8 MIMO antennas are given in Fig. 11. As shown in Fig. 11(a), the S_{11}

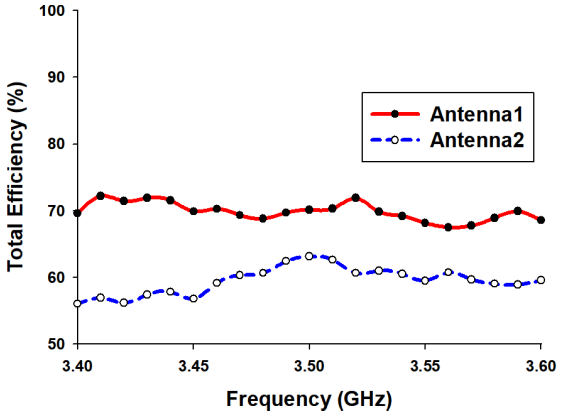

FIGURE 14. Measured total efficiencies of the fabricated 8 × 8 MIMO antennas.

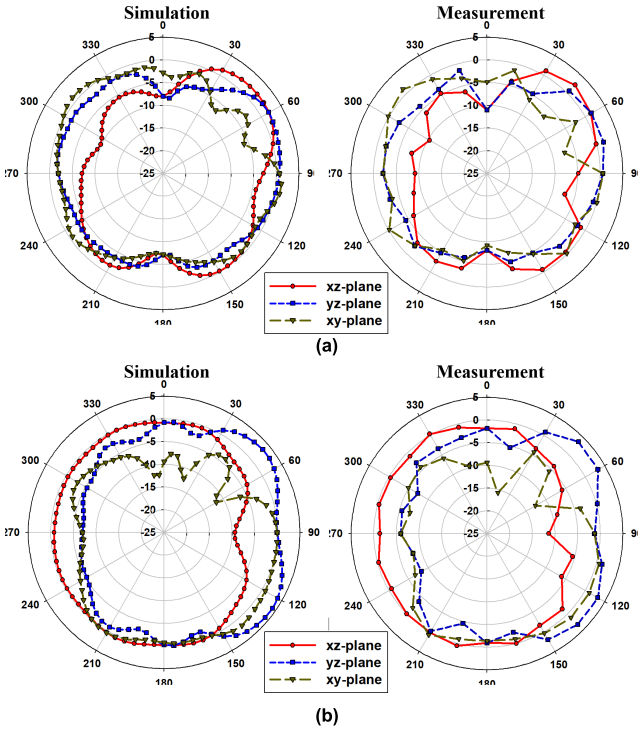

FIGURE 15. Simulated and measured radiation patterns of the proposed 8 × 8 MIMO antennas at 3.5 GHz: (a) Antenna-1, and (b) Antenna-2.

and S_{22} curves indicate that the antennas can fully cover the 3.5 GHz band for 5G applications. Furthermore, the transmission coefficients are presented in Figs. 11(b) and (c), where it can be seen that the isolation between any two antenna elements is over 16 dB. Since the spatial distance between each two MIMO antenna sets is over one wavelength, the isolation performance of the proposed MIMO antenna system is not sensitive to this distance. Therefore, the proposed MIMO antennas can be promisingly employed in current and future terminal devices for 5G applications, having advantages of compact volume, easy fabrication, and high isolation property.

TABLE 1. Comparisons with previously published literature.

Ref.	Decoupling method	Isolation(dB)	Spacing (edge-to-edge)	-6dB impedance bandwidth	Complexity
[7]	Decoupling network	>11.8	<5mm	175 MHz (3415–3590 MHz)	Need for lumped components
[9]	Hybrid decoupling (neutralization line and ground slot)	>15	17mm	300 MHz (3300-3600MHz)	Complex
[10]	Additional resonator	>20	30mm	>200MHz	Need for complex and large-sized decoupling structures
[15]	Spatial arrangement	>10	17mm	>200MHz	Simple
[18]	Pattern diversity	>10	Integrated	>200MHz	Complicated try-and-error process
[22]	Pattern diversity	>18	Integrated	>200MHz	Difficult fabrication
This work	Self-decoupling	>20	Integrated	>300MHz	Simple

B. FABRICATION AND MEASUREMENT

To further validate the proposed technique, the proposed 8 × 8 MIMO antennas were fabricated, and its prototype is pictured in Fig. 12. Moreover, the fabricated 8 × 8 MIMO antennas were then tested using a network analyzer and in a 6 m × 3 m × 3 m three-dimensional (3D) CTIA OTA anechoic chamber to derive the measured impedance characteristics and far-field parameters.

First, the measured reflection coefficients and transmission coefficients are presented in Fig. 13. It can be verified that the measured results are similar to the simulated ones, and the slight difference between measurement and simulation may be attributed to the fabrication error and the soldered semi-rigid cables. Furthermore, the antennas produced sufficient impedance bandwidths that can fully cover the target frequency band (see Fig. 13(a)). Meanwhile, the measured transmission coefficient between each two antenna elements is lower than −17 dB (see Figs. 13(b) and (c)), satisfying the engineering requirement in practical scenarios.

Additionally, the measured total efficiencies are plotted in Fig. 14, where it can be observed that high efficiencies over 56% can be obtained over the frequency range from 3.4 to 3.6 GHz, indicating their high radiation performances and feasibility in practical applications. Furthermore, the far-field radiation patterns at 3.5 GHz are also displayed in the *xz*-, *yz*-, and *xy*-planes, as shown in Fig. 15. The maximum gains produced by Antenna 1 and Antenna 2 direct against each other, and this is an important feature that can guarantee excellent diversity performance of MIMO antennas. Herein, correlation is an essential parameter to identify the diversity performance of MIMO antennas, which can be computed by considering the amplitude, phase, and polarization of the 3D far-field radiation patterns [36]. Therefore, the envelope correlation coefficient (ECC) ρ_e of the proposed MIMO antennas are obtained by measuring the 3D far-field radiation pattern and plotted in Fig. 16. It can be observed that all the measured ECC values are below 0.1, which is much lower than the acceptable criterion ($\rho_e < 0.5$) in mobile applications, indicating their extraordinary diversity performances. Therefore, the proposed technique is a simple yet effective method that can achieve high isolation and low correlation simultaneously, suitable for the 5G MIMO applications in current and future terminal devices.

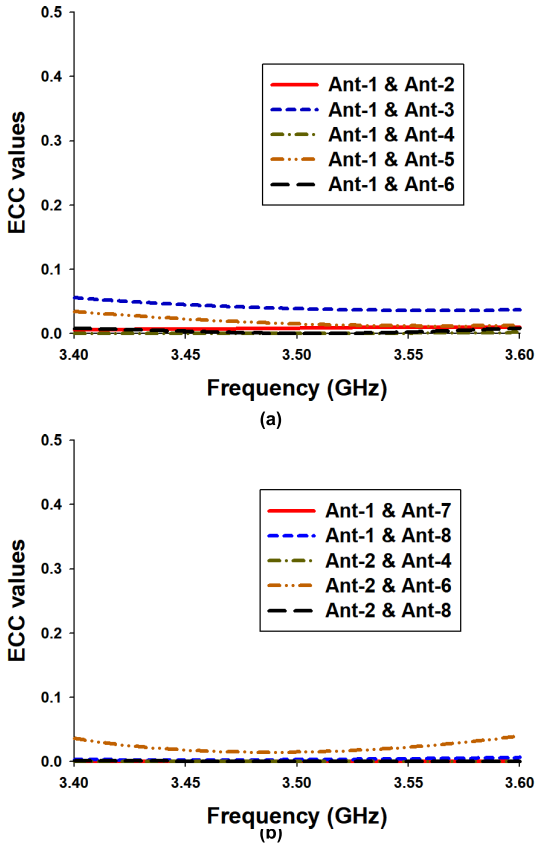

FIGURE 16. Measured ECC values of the fabricated 8 × 8 MIMO antennas.

C. COMPARISON

A comparison table with the state-of-the-art MIMO antennas is presented to validate the novelty and advantages of

the proposed technique. As shown in Table 1, the self-decoupling technique has superiority in compactness and simple implementation when compared to the aforementioned decoupling techniques, such as decoupling network, additional resonators, and spatial arraignment. The proposed self-decoupled MIMO set exhibits comparable isolation and bandwidth performance but has a simpler implementation compared to [18] and [22].

IV. CONCLUSION

In this paper, a simple and compact self-decoupled MIMO antenna set is accomplished by merely assembling a loop antenna and a ground-radiation antenna. It has been demonstrated that the high isolation property is obtained due to the orthogonality between the equivalent electric-current element of the loop antenna and the equivalent magnetic-current element of the ground-radiation antenna. This orthogonality between the two antennas is the fundamental feature that allows the successful construction of various implementation cases to suit for different application scenarios.

The 8 × 8 MIMO antennas for 5G applications are investigated in both simulation and measurement. The antennas can produce wide impedance bandwidths and measured total efficiencies over 56%. Meanwhile, the measured ECC values between any two antenna elements are below 0.1, which can also be confirmed from their complementary radiation patterns. Therefore, the proposed MIMO antenna set can be a promising candidate for current and future 5G terminal devices, having advantages of high integration, low profile, easy implementation, as well as excellent radiation performance and diversity performances. Furthermore, further study is now undergoing, such as the multiband self-decoupled antenna sets.

ACKNOWLEDGMENT

(Haiyan Piao and Yunnan Jin contributed equally to this work.)

REFERENCES

[1] A. Sibille, C. Oestges, and A. Zanella, *MIMO: From Theory to Implementation*. San Diego, CA, USA: Academic, 2011.

[2] E. Björnson, E. G. Larsson, and T. L. Marzetta, "Massive MIMO: Ten myths and one critical question," *IEEE Commun. Mag.*, vol. 54, no. 2, pp. 114–123, Feb. 2016.

[3] F. Boccardi, R. W. Heath, A. Lozano, T. L. Marzetta, and P. Popovski, "Five disruptive technology directions for 5G," *IEEE Commun. Mag.*, vol. 52, no. 2, pp. 74–80, Feb. 2014.

[4] M. Agiwal, A. Roy, and N. Saxena, "Next generation 5G wireless networks: A comprehensive survey," *IEEE Commun. Surveys Tuts.*, vol. 18, no. 3, pp. 1617–1655, 3rd Quart., 2016.

[5] WRC-15 Press Release. (Nov. 27, 2015). *World Radiocommunication Conference Allocates Spectrum for Future Innovation*. [Online]. Available: http://www.itu.int/net/pressoffice/press_releases/2015/56.aspx

[6] M.-Y. Li, Y.-L. Ban, Z.-Q. Xu, J. Guo, and Z.-F. Yu, "Tri-polarized 12-antenna MIMO array for future 5G smartphone applications," *IEEE Access*, vol. 6, pp. 6160–6170, 2018.

[7] C. Deng, D. Liu, and X. Lv, "Tightly arranged four-element MIMO antennas for 5G mobile terminals," *IEEE Trans. Antennas Propag.*, vol. 67, no. 10, pp. 6353–6361, Oct. 2019.

[8] J. Guo, L. Cui, C. Li, and B. Sun, "Side-edge frame printed eight-port dual-band antenna array for 5G smartphone applications," *IEEE Trans. Antennas Propag.*, vol. 66, no. 12, pp. 7412–7417, Dec. 2018.

[9] W. Jiang, B. Liu, Y. Cui, and W. Hu, "High-isolation eight-element MIMO array for 5G smartphone applications," *IEEE Access*, vol. 7, pp. 34104–34112, 2019.

[10] H. Xu, H. Zhou, S. Gao, H. Wang, and Y. Cheng, "Multimode decoupling technique with independent tuning characteristic for mobile terminals," *IEEE Trans. Antennas Propag.*, vol. 65, no. 12, pp. 6739–6751, Dec. 2017.

[11] L. Cui, J. Guo, Y. Liu, and C.-Y.-D. Sim, "An 8-element dual-band MIMO antenna with decoupling stub for 5G smartphone applications," *IEEE Antennas Wireless Propag. Lett.*, vol. 18, no. 10, pp. 2095–2099, Oct. 2019.

[12] W. Jiang, Y. Cui, B. Liu, W. Hu, and Y. Xi, "A dual-band MIMO antenna with enhanced isolation for 5G smartphone applications," *IEEE Access*, vol. 7, pp. 112554–112563, 2019.

[13] Y. Li, C.-Y.-D. Sim, Y. Luo, and G. Yang, "12-port 5G massive MIMO antenna array in sub-6 GHz mobile handset for LTE bands 42/43/46 applications," *IEEE Access*, vol. 6, pp. 344–354, 2018.

[14] Y. Li, C.-Y.-D. Sim, Y. Luo, and G. Yang, "Multiband 10-antenna array for Sub-6 GHz MIMO applications in 5-G smartphones," *IEEE Access*, vol. 6, pp. 28041–28053, 2018.

[15] Y. Li, C.-Y.-D. Sim, Y. Luo, and G. Yang, "4G/5G multiple antennas for future multi-mode smartphone applications," *IEEE Access*, vol. 6, pp. 28041–28053, 2019.

[16] Y. Liu, A. Ren, H. Liu, H. Wang, and C.-Y.-D. Sim, "Eight-port MIMO array using characteristic mode theory for 5G smartphone applications," *IEEE Access*, vol. 7, pp. 45679–45692, 2019.

[17] X. Zhang, Y. Li, W. Wang, and W. Shen, "Ultra-wideband 8-port MIMO antenna array for 5G metal-frame smartphones," *IEEE Access*, vol. 7, pp. 72273–72282, 2019.

[18] K.-L. Wong, C.-Y. Tsai, and J.-Y. Lu, "Two asymmetrically mirrored gap-coupled loop antennas as a compact building block for eight-antenna MIMO array in the future smartphone," *IEEE Trans. Antennas Propag.*, vol. 65, no. 4, pp. 1765–1778, Apr. 2017.

[19] N. O. Parchin, Y. I. A. Al-Yasir, A. H. Ali, I. Elfergani, J. M. Noras, J. Rodriguez, and R. A. Abd-Alhameed, "Eight-element dual-polarized MIMO slot antenna system for 5G smartphone applications," *IEEE Access*, vol. 7, pp. 15612–15622, 2019.

[20] Z. Ren and A. Zhao, "Dual-band MIMO antenna with compact self-decoupled antenna pairs for 5G mobile applications," *IEEE Access*, vol. 7, pp. 82288–82296, 2019.

[21] A. Ren, Y. Liu, and C.-Y.-D. Sim, "A compact building block with two shared-aperture antennas for eight-antenna MIMO array in metal-rimmed smartphone," *IEEE Trans. Antennas Propag.*, vol. 67, no. 10, pp. 6430–6438, Oct. 2019.

[22] A. Ren, Y. Liu, H.-W. Yu, Y. Jia, C.-Y.-D. Sim, and Y. Xu, "A high-isolation building block using stable current nulls for 5G smartphone applications," *IEEE Access*, vol. 7, pp. 170419–170429, 2019.

[23] C.-Z. Han, L. Xiao, Z. Chen, and T. Yuan, "Co-located self-neutralized handset antenna pairs with complementary radiation patterns for 5G MIMO applications," *IEEE Access*, vol. 8, pp. 73151–73163, 2020.

[24] Y. Liu, H. H. Kim, J. Lee, and H. Kim, "Ground radiation method using slot with coupling capacitors," *Electron. Lett.*, vol. 49, no. 7, pp. 447–448, Mar. 2013.

[25] Y. Liu, H.-H. Kim, and H. Kim, "Loop-type ground radiation antenna for dual-band WLAN applications," *IEEE Trans. Antennas Propag.*, vol. 61, no. 9, pp. 4819–4823, Sep. 2013.

[26] L. Qu, R. Zhang, and H. Kim, "High-sensitivity ground radiation antenna system using an adjacent slot for Bluetooth headsets," *IEEE Trans. Antennas Propag.*, vol. 63, no. 12, pp. 5903–5907, Dec. 2015.

[27] L. Qu, H. Kim, and R. Zhang, "Decoupling between ground radiation antennas with ground-coupled loop-type isolator for WLAN applications," *IET Microw., Antennas Propag.*, vol. 10, no. 5, pp. 546–552, Apr. 2016.

[28] Z. Zahid and H. Kim, "Analysis of a loop type ground radiation antenna based on equivalent circuit model," *IET Microw., Antennas Propag.*, vol. 11, no. 1, pp. 23–28, Jan. 2017.

[29] W. Lei, H. Chu, and Y.-X. Guo, "Design of a circularly polarized ground radiation antenna for biomedical applications," *IEEE Trans. Antennas Propag.*, vol. 64, no. 6, pp. 2535–2540, Jun. 2016.

[30] L. Qu, H. Piao, Y. Qu, H.-H. Kim, and H. Kim, "Circularly polarised MIMO ground radiation antennas for wearable devices," *Electron. Lett.*, vol. 54, no. 4, pp. 189–190, Feb. 2018.

[31] H. Piao and L. Qu, "A self-decoupled MIMO antenna system," CN Patent 202 010 019 168 2, Jan. 8, 2020.

[32] M. Zheng, H. Wang, and Y. Hao, "Internal hexa-band folded monopole/dipole/loop antenna with four resonances for mobile device," *IEEE Trans. Antennas Propag.*, vol. 60, no. 6, pp. 2880–2885, Jun. 2012.
[33] Y.-L. Ban, Y.-F. Qiang, Z. Chen, K. Kang, and J.-H. Guo, "A dual-loop antenna design for hepta-band WWAN/LTE metal-rimmed smartphone applications," *IEEE Trans. Antennas Propag.*, vol. 63, no. 1, pp. 48–58, Jan. 2015.
[34] A. Zhao and Z. Ren, "Wideband MIMO antenna systems based on coupled-loop antenna for 5G N77/N78/N79 applications in mobile terminals," *IEEE Access*, vol. 7, pp. 93761–93771, 2019.
[35] C. A. Balanis, *Antenna Theory: Analysis and Design*, 4th ed. Hoboken, NJ, USA: Wiley 2016.
[36] R. G. Vaughan and J. B. Andersen, "Antenna diversity in mobile communications," *IEEE Trans. Veh. Technol.*, vol. 36, no 4, pp. 149–172, Nov. 1987.

HAIYAN PIAO received the B.Sc. degree in communication engineering from Yanbian University, China, in 2013, and the M.Sc. degree from the Department of Microwave Engineering, Hanyang University, Seoul, South Korea, in 2017.

Her research interests are antenna design, MIMO, 5G communications, and the IoT.

YUNNAN JIN (Member, IEEE) received the B.S. degree in telecommunication engineering from the Yanbian University of Science and Technology, Yanji, China, in 2013, and the Ph.D. degree from the Department of Electronics and Computer Engineering, Hanyang University, Seoul, South Korea, in 2019.

He is an author of over 15 international articles and conference papers, and an inventor of six patents. He serves as a Reviewer for the *Microwave and Optical Technology Letters* and the *International Journal of Electronics and Communications*. His current research interests include antenna theory and design, especially for 4G/5G communications, massive MIMO, mmWave, and various high-gain antenna.

LONGYUE QU (Member, IEEE) received the B.S. degree in electronic engineering from Yanbian University, China, in 2013, and the M.S. and Ph.D. degrees in electromagnetics and microwave engineering from Hanyang University, Seoul, South Korea, in 2015 and 2018, respectively.

Since 2020, he has been a Professor with the School of Electronics & Information Engineering, Nanjing University of Information Science & Technology (NUIST), China. He is currently an Assistant Research Professor with Hanyang University. He is the author of more than 40 articles, and more than 30 inventions. He serves as a reviewer for several international journals and conferences. His current research interests include antenna theory and design, metamaterial-based antenna technology, millimeter-wave arrays, and RF circuits.

Dr. Qu was a recipient of the Korean Government Scholarship Award and China Scholarship Council (CSC). His research is listed in the Top 100 National Research and Development Excellence Award in 2015. He also serves as an Editorial Board Member in the *International Journal of Sensors* and *Wireless Communications and Control*.